Vascular invasion in hepatocellular carcinoma: is there a correlation with MRI?

[1]N GRIFFIN, MD, FRCR, ^{2}H ADDLEY, FRCR, [2]E SALA, PhD, FRCR, [2]A S SHAW, FRCR, [2]L A GRANT, FRCR, ^{3}H ELDALY, MRCPath, [3]S E DAVIES, MRCPath, [4]T PREVOST, MSc, PhD, [5]G J ALEXANDER, MD, FRCP and [2]D J LOMAS, FRCR

[1]Department of Radiology, Guys and St Thomas' Hospital, London, UK, [2]Department of Radiology, Addenbrooke's Hospital, Cambridge, UK, [3]Department of Histopathology, Addenbrooke's Hospital, Cambridge, UK, [4]Centre for Applied Medical Statistics, Addenbrooke's Hospital, Cambridge, UK, and [5]Department of Hepatology, Addenbrooke's Hospital, Cambridge, UK

Objective: Hepatocellular carcinoma (HCC) is one of the commonest malignancies worldwide. Prognosis is predicted by size at diagnosis, vascular invasion and tumour proliferation markers. This study investigates if MRI features of histologically proven HCCs correlate with vascular invasion.

Methods: Between 2006 and 2008, 18 consecutive patients, with a total of 27 HCCs, had comprehensive MRI studies performed at our institution within a median of 36 days of histology sampling. Each lesion was evaluated independently on MRI by 3 radiologists (blinded to both the radiology and histopathology reports) using a 5-point confidence scale for 23 specific imaging features. The mean of the rating scores across readers was calculated to determine interobserver consistency. The most consistent features were then used to examine the value of features in predicting vascular invasion, using a χ^2 test for trend, having eliminated those features without sufficient variability.

Results: 22 of the 23 imaging features showed sufficient variability across lesions. None of these significantly correlated with the presence of vascular invasion, although a trend was identified with the presence of washout in the portal venous phase on MRI and the median size of lesions, which was greater with vascular invasion.

Conclusion: This study suggests that no single MRI feature accurately predicts the presence of vascular invasion in HCCs, although a trend was seen with the presence of washout in the portal venous phase post gadolinium. Larger prospective studies are required to investigate this further.

Hepatocellular carcinoma (HCC) is one of the commonest malignancies worldwide, either arising *de novo* or on a background of cirrhosis. The incidence in Western countries is rising owing to increasing rates of alcoholic liver disease and hepatitis C infection. Untreated, the 5-year survival rate for symptomatic HCC is less than 5% [1]. At present, surgery is the only potentially curative treatment for HCC with options including either a partial hepatectomy or orthotopic liver transplantation (OLT). Following resection there is a 5-year survival rate of 40–50% [2] with a cumulative 5-year recurrence rate between 75 and 100% [3]. The 5-year survival rate in patients with cirrhosis following transplantation of small (<2 cm) HCC is up to 80% [4]. However, the use of OLT is limited owing to the lack of donor livers. Regional therapies such as transcatheter arterial chemoembolisation [5] and percutaneous radiofrequency ablation [6] may improve prognosis. The value of neo-adjuvant and adjuvant chemotherapy and immunotherapy in prolonging survival remains controversial [7, 8]. However, a recent study evaluating sorafenib, a multikinase inhibitor,

in patients with advanced HCC has shown an increased median overall survival of 2.8 months over a placebo [9].

Studies of patients with explanted liver for end-stage cirrhosis have shown that MRI, with the use of dynamic gadolinium-enhanced sequences, has a moderate sensitivity for the detection of HCC of between 55 and 91% [10–12] and specificity between 55 and 86% [11–13]. The sensitivity is lower with lesions <2 cm in size [11–13]. In patients with cirrhosis, HCC is thought to develop as part of a spectrum of de-differentiation from regenerative nodule through to low-grade dysplastic nodule, high-grade dysplastic nodule, then to frankly malignant. Early diagnosis using non-invasive imaging leads to an improved prognosis but at present, unless biopsy is performed, only lesion size is used to determine patient management in those where gross vascular involvement or metastatic spread precludes curative treatment.

Several factors predicting outcome have been identified including tumour pathological factors (such as size, stage, grade, the presence of vascular invasion, portal vein tumour thrombus and intrahepatic metastases) [14, 15], the patient's hepatitis status, the patient's functional liver reserve [16] and the serum α-fetoprotein level [17]. Overall, one of the most strongly correlated factors is the presence or absence of vascular invasion. There is a

Address correspondence to: Dr Nyree Griffin, Department of Radiology, Guys and St Thomas' Hospital, Westminster Bridge Road, London SE1 7EH, UK. E-mail: nyreegriffin100@gmail.com

4.4- and 15-fold increased risk of recurrence following OLT for HCC in patients with micro- or macrovascular invasion, respectively [18].

The aims of this retrospective study were twofold. First to identify the interobserver variability of MRI features for patients with histologically proven HCC, and second to determine if there was a correlation between imaging features on MRI and histologically defined vascular invasion; these MRI features could then serve as a surrogate marker of prognosis. There has been little literature to date attempting to correlate MRI features with microvascular invasion.

Methods and materials

A written ethics committee waiver was obtained for this retrospective study. Between 2006 and 2008, 18 consecutive patients, with tumours <3.5 cm, had undergone a pre-operative comprehensive MRI study using the same protocol at our institution within a median of 36 days (interquartile range 24.3–59.5 days) of histology sampling. Patients were identified from the histopathological and radiology databases. This group then formed the basis for our study.

MRI protocol

MRI was performed on a 1.5 T whole-body MRI scanner (Excite; GE Healthcare, Milwaukee, WI) with a multi-channel receiver array coil. Breath-hold effective echo time (TE_{eff}) 60 ms and TE_{eff} 160 ms T_2 weighted single shot fast spin echo images [SSFSE; matrix 256×256; repetition time (TR) 1100–1400 ms; slice thickness/gap 10/0 mm; acquisition time 12–18 s], T_1 weighted in- and out-of-phase fast spoiled gradient echo (FSPGR; matrix 256×128; TR 180 ms; echo time (TE) 2.25/4.5 ms; slice thickness/gap 10/0 mm; acquisition time 18 s) and respiratory triggered T_2 weighted fat suppressed TE_{eff} 65 ms multishot fast spin echo (FSE; matrix 256×320; slice thickness/gap 8/2 mm; acquisition time 4–7 min) sequences were obtained. These were supplemented with pre- and post-intravenous gadolinium (Gd)-diethylenetriaminepentacetic acid fluoroscopically triggered multiphase (arterial, portal, 90 s and 300 s) volume interpolated fat-suppressed three-dimensional (3D) T_1 weighted imaging (liver acquisition with volume acquisition; matrix 284×192; TR 3.4 ms; TE 1.5 ms, slice thickness/gap 5/0 mm; acquisition time 16–20 s).

Histopathology

Histopathology specimens consisted of liver explants ($n=12$), liver resection ($n=4$) or biopsy of focal lesion ($n=2$). Analysis was performed by two histopathologists with more than 10 years of subspecialty experience. Each specimen was fixed in 10% neutral formalin and embedded in paraffin. For patients with explanted livers, the livers were cut into sequentially oriented slices (from superior to inferior) of 1 cm thickness. The size, number and location of tumours were documented. Thin sections were stained routinely with haematoxylin and eosin. The presence of microvascular invasion was recorded for both liver explants and liver biopsy specimens.

Table 1. Significance values for prediction of vascular invasion on histopathology

Sequence	Imaging feature	Lesion feature[a]	Mean discrepancy between readers	Rank of mean discrepancy	*p*-value[b]
T_1	1	**Increased signal within**	0.68	**3**	**0.16**
	2	Decreased signal within	1.9	22	0.59
	3	Heterogeneity within	1.84	21	0.82
	4	**Irregular margin**	1.06	**6**	0.9
	5	Presence of a rim	1.52	16	0.48
I/O phase T_1W	6	**Presence of fat within**	0.71	**4**	0.89
T_2	7	Increased signal within	1.74	18.5	0.21
	8	**Decreased signal within**	1.19	**8**	0.71
	9	Heterogeneity within	2	23	0.35
	10	Irregular margin	1.74	18.5	0.67
	11	**Presence of a rim**	1.26	**9.5**	0.96
T_1 arterial	12	Arterial enhancement	0	1	n/a[c]
	13	**Heterogeneous enhancement**	0.58	**2**	1
	14	**Irregular margin**	1.39	**11**	0.7
	15	Presence of a rim	1.42	13	0.18
T_1 portal	16	**Presence of washout**	1.26	**9.5**	**0.09**
	17	Heterogeneous washout	1.77	20	0.18
	18	Irregular margin	1.55	17	0.86
	29	Presence of a rim	1.42	13	0.21
T_1 delayed	20	**Presence of washout**	1	**5**	**0.13**
	21	Heterogeneous washout	1.42	13	0.2
	22	Irregular margin	1.45	15	0.5
	23	**Presence of a rim**	1.16	**7**	0.44

I/O phase T_1W, T_1 weighted in and out of phase.
[a]Features in bold are the 10 most consistent imaging features amongst the 3 readers (ranked 2–11), after the most consistent imaging feature (arterial enhancement) has been excluded for insufficient variability.
[b]*p*-values in bold are those features out of the 10 most consistent that have *p*<0.2 for vascular invasion.
[c]This feature (arterial enhancement) was excluded from the analysis as there was insufficient variability between the three readers and across all lesions.
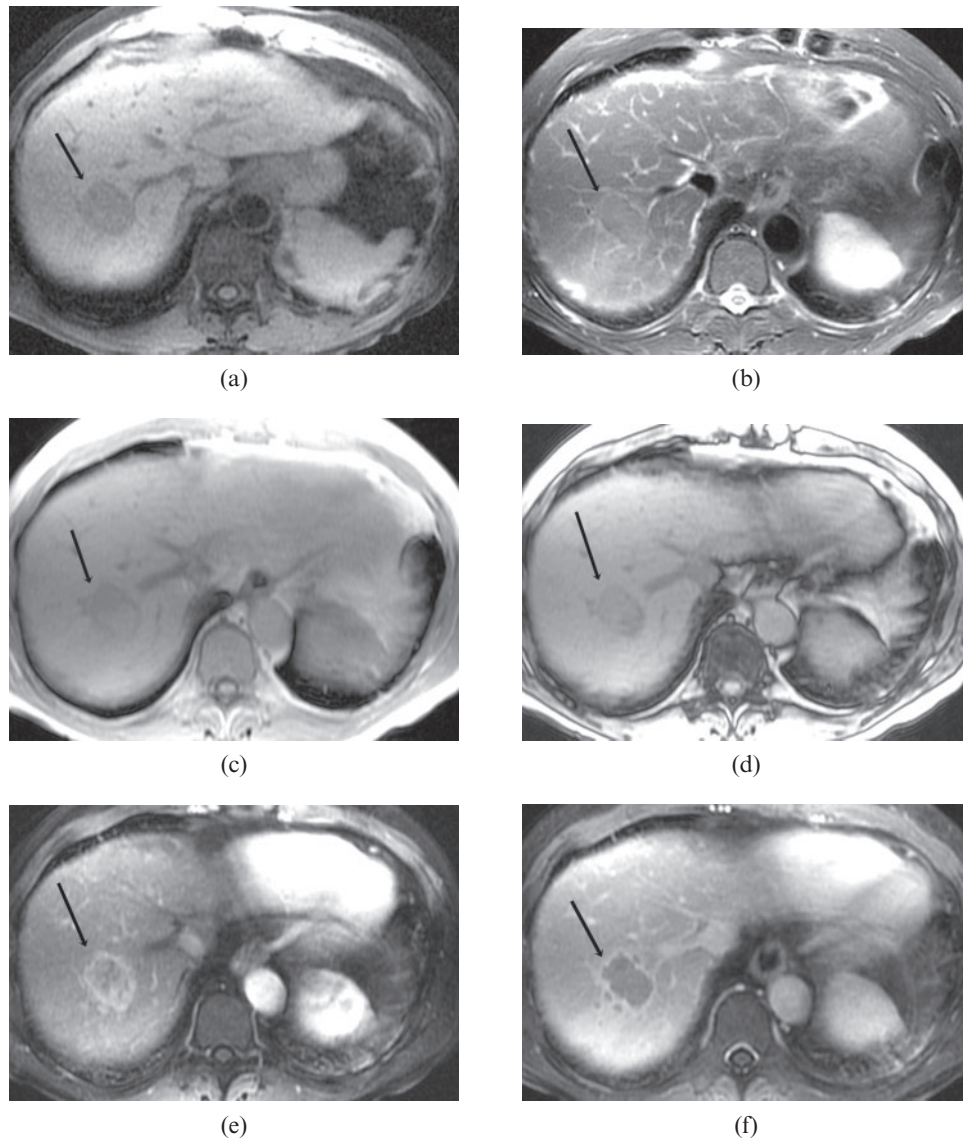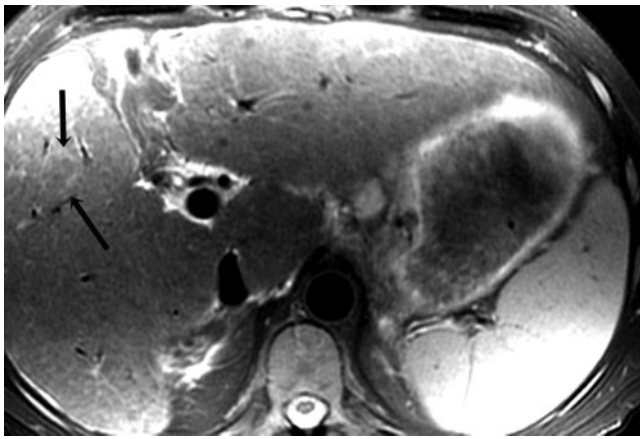
Figure 1. Histologically proven hepatocellular carcinoma in segment 7 of the liver in a 72-year-old male with relatively normal background liver texture: (a) axial T_1 weighted image shows the lesion to be homogeneously hypointense to the rest of the liver with a well-defined margin (arrow); (b) axial T_2 weighted image shows the lesion to be mildly hyperintense to the rest of the liver with a well-defined hyperintense rim (arrow); (c,d) axial T_1 in- and out-of-phase images show signal dropout on the out-of-phase images in part of the lesion, in keeping with the presence of fat (arrow); (e) arterial T_1 weighted image shows heterogeneous enhancement of the lesion with irregular rim enhancement (arrow); (f) portal venous T_1 weighted image shows central washout with remaining irregular rim enhancement (arrow).

MRI interpretation

MR studies were reviewed independently on picture archiving and communication system workstations, by 3 radiologists, with Readers 1, 2 and 3 having 15, 7 and 4 years of specialist experience in hepatobiliary imaging, respectively. All were blinded to both the radiology and the histopathology reports. The three readers were instructed to review only specific histologically proven HCCs on the data set, which had been identified in advance by correlation with histopathology reports by a separate radiologist. For each of the MRI sequences, the reader first had to determine whether the lesion was visible using binary scoring. In addition, the reader had to determine if hepatic vascular thrombus was present on any of the sequences. Size of the lesion was recorded based on the arterial phase post-gadolinium images. Following the advice of the hospital statistician, the reader then evaluated these lesions for 23 specific imaging features (column 3 in Table 1, Figures 1–4) using a 5-point confidence rating score. Signal intensity of the lesion was compared with the background liver signal intensity to determine the presence of high or low signal intensity within the tumour. A score of 1 indicated that the feature was definitely not present, a score of 5 indicated that the feature was definitely present and a score of 3 indicated that the feature was indeterminate. A score of 2 or 4 meant that the reader felt that the feature was probably absent or probably present, respectively. For lesions that were not originally detectable on one particular sequence a score of 1 was automatically assigned for all features related to this MRI sequence.
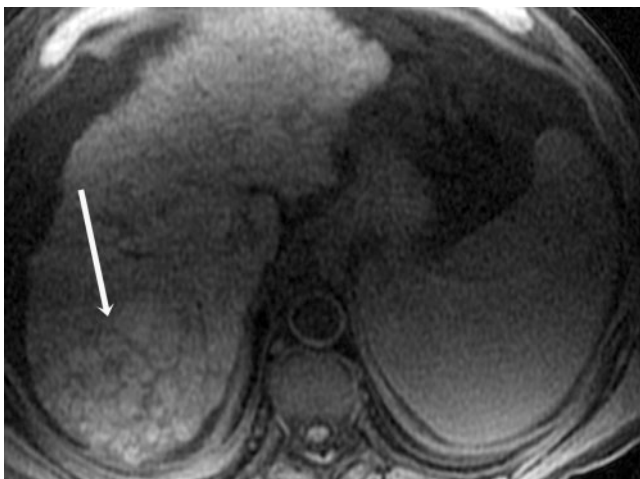
Figure 2. Histologically proven hepatocellular carcinoma in segment 5 of the liver in a 54-year-old male; axial T_2 weighted image shows the lesion to be atypically hypointense to the rest of the liver with a well-defined hyperintense rim (arrows).

Background liver texture was also assessed for each patient using a similar five-point scale, where 1 denoted that the liver was definitely normal and 5 represented definitely abnormal. In order to ensure that there was reader agreement for the criteria used to define the 23 imaging features, a training set of 10 MRI studies in patients thought to have likely HCC lesions on imaging but no established histological diagnosis of HCC was first reviewed by the 3 radiologists in consensus.

Statistical analysis

The data were analysed in several ways, after seeking advice from the hospital statistician. First, the number of lesions detected on each of the MRI sequences was calculated for each reader. Second, in order to determine the MRI characteristics of the lesions, the mean and standard deviation (SD) of the confidence rating score for each imaging feature across all lesions and across the

Figure 3. Histologically proven hepatocellular carcinoma in segment 7 of the liver in a 61-year-old male; axial T_1 weighted image shows the lesion to be heterogeneously hyperintense to the rest of the liver (arrow).
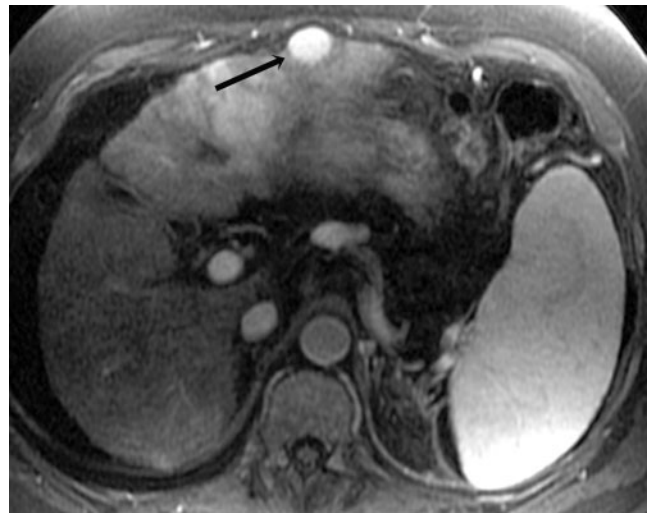
Figure 4. Histologically proven hepatocellular carcinoma in segment 3 of the liver in a 56-year-old male; arterial T_1 weighted image shows homogeneous arterial enhancement (arrow).

three readers were calculated. These mean scores were then represented as a graph with the score first rescaled so that score 3 acted as the new baseline; hence an original score of 1 would be readjusted to -2 and an original score of 5 would be equivalent to $+2$.

Third, for each imaging feature and lesion, discrepancy was calculated as the range in score across the three readers. The mean discrepancy across the lesions was then used as an overall measure for reader consistency for each feature and used to examine the value of imaging features in predicting vascular invasion using a χ^2 test for trend. Those features ($n=1$) without sufficient variability (*i.e.* where the imaging feature for the lesion was rated as present or absent by all three readers) were initially eliminated from the analysis.

Using a one-sample *t*-test, the size of each lesion as measured by each reader was compared with the final histological size to determine concordance. Finally, using the Mann–Whitney *U*-test, comparison was made between the median size of lesions on histopathology where vascular invasion was present and the median size of lesions where vascular invasion was absent. For all statistical analyses, $p<0.05$ was considered significant.

Results

There were 18 male patients (median age 56.4 years, interquartile range 53.4–61.4 years) with a histopathological diagnosis of HCC. Patient demographics and aetiology are shown in Table 2. There was a total of 27 histologically proven tumours, with 21 lesions being in the right lobe and 6 in the left lobe. These were either moderate or poorly differentiated. 13 patients had solitary lesions, the remainder had multiple.

The median histological size of the lesions was 22 mm (interquartile range 15.8–25.3 mm). The median interval between the MRI study and histopathological diagnosis was 36 days (interquartile range 24.3–59.5 days). Nine of the lesions demonstrated vascular invasion on

Table 2. Patient demographics and aetiology of hepatocellular carcinoma

Patient	Gender	Age (years)	Aetiology
1	M	34	HBV
2	M	53	HCV
3	M	54	HCV
4	M	72	NASH and HCV
5	M	56	HCV
6	M	45	ALD
7	M	45	HCV
8	M	61	ALD
9	M	61	ALD
10	M	64	ALD
11	M	68	NASH
12	M	46	HBV
13	M	59	HCV
14	M	53	HCV
15	M	56	Cryptogenic cirrhosis
16	M	58	HCV
17	M	52	HCV
18	M	65	HCV

ALD, alcoholic liver disease; HBV, hepatitis B virus; HCV, hepatitis C virus; M, male; NASH, non-alcoholic steatohepatitis.

histopathology. No thrombus was demonstrated in any of the major hepatic or portal veins on MRI. Background liver texture was considered abnormal in the majority of cases (in 14 patients for Reader 1 and in 13 patients for Readers 2 and 3) with a mean unadjusted confidence rating score ($\pm$SD) across all lesions and readers of 4.6 ± 0.88. The median size of the lesion as determined by the readers was not significantly different from the median size of the lesion on histopathology.

Figure 5 demonstrates the number of lesions detected on each MR sequence for each of the three readers. Apart from the arterial sequence, Reader 2 identified a greater number of lesions on each of the sequences than the other two readers. Figure 6 shows the mean adjusted

confidence rating score and standard deviation for all 27 lesions across the 3 readers, for each of the 23 imaging features. Table 1 illustrates the mean discrepancy between all three readers across all lesions for each imaging feature. The most consistent imaging features (mean discrepancy of ≤ 1 between readers, ranked 1–5 in Table 1) were on T_1 weighted imaging and included the presence of arterial enhancement, heterogeneity on arterial enhancement, washout on delayed gadolinium imaging and the absence of increased signal intensity. Another consistent feature included the absence of fat on the in- and out-of-phase imaging. Inconsistent features (mean discrepancy >1.5) were mainly on T_2 weighted imaging, including the presence of increased signal intensity, irregular margin and lesion heterogeneity.

One feature (*i.e.* presence of arterial enhancement) was consistently reported by all three readers (mean discrepancy=0); this showed insufficient variability across all lesions and thus could not be used as a feature to predict the presence or absence of vascular invasion. The significance values for predicting vascular invasion for the remaining 22 features are shown in Table 1. Out of the 10 most consistent imaging features (excluding arterial enhancement), those features with a p-value <0.2 included the lack of increased signal intensity within the lesion on T_1 weighted images, and the presence of washout in the portal venous and delayed phases. A trend towards vascular invasion on histopathology was seen with the presence of washout in the portal venous phase on MRI (p=0.09). Out of those lesions that demonstrated no washout in the portal venous phase, 14% (2/14) had vascular invasion compared with 54% (7/13) in those lesions that did demonstrate washout.

Lesions where no vascular invasion was present had a median size on histopathology of 19.2 mm compared with 23 mm for lesions where vascular invasion was present (p=0.18).
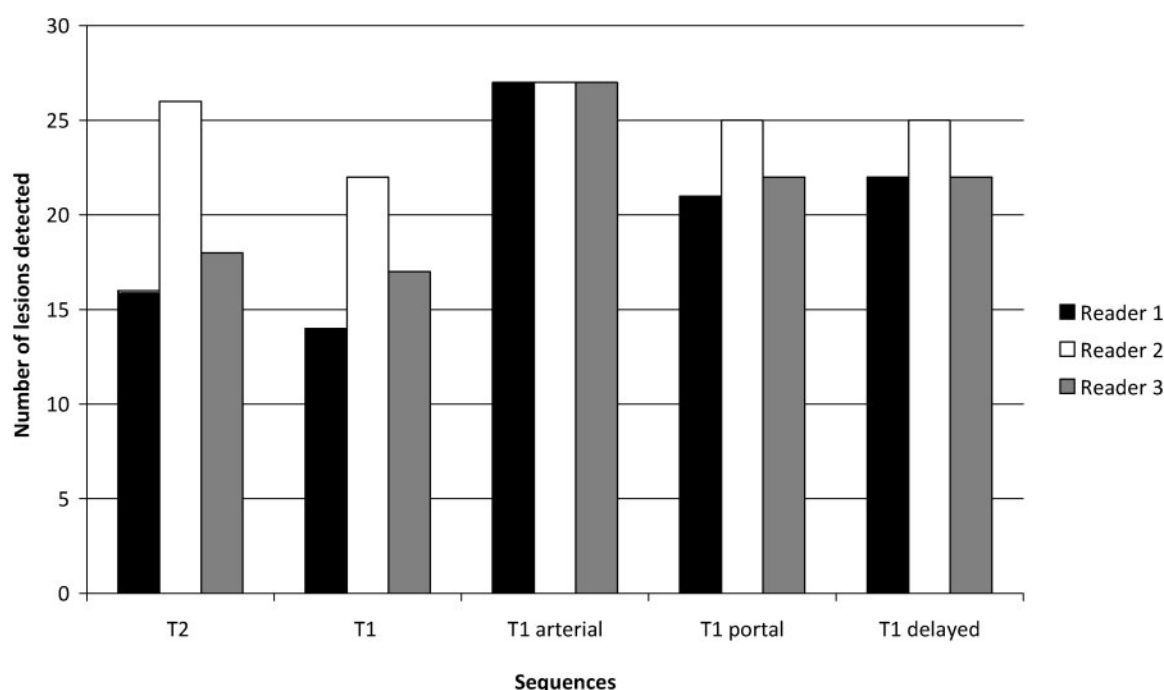
Figure 5. Bar chart demonstrating number of lesions detected on each MRI sequence by each reader.
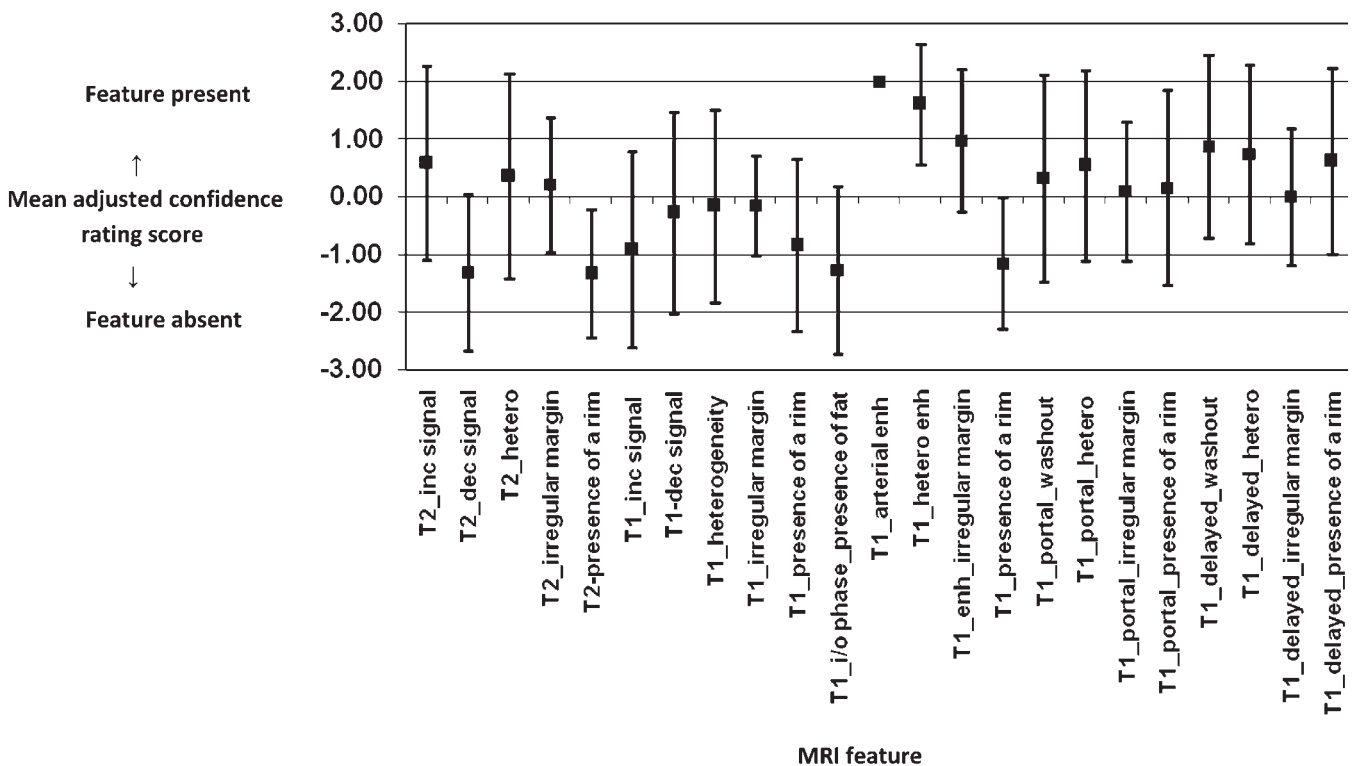
Figure 6. Graph showing mean adjusted confidence rating score ($\pm$standard deviation) for each feature across all 27 lesions and all 3 readers.

Discussion

The 23 imaging features chosen for this study were based on established literature where recognised features of HCC include heterogeneous signal intensity on T_1 and T_2 weighted images, increased signal intensity on T_2 weighted images, arterial phase enhancement, "washout" in the portal or delayed phase, the presence of a capsule and portal vein thrombosis [19, 20]. Other features that have been described but that were not assessed in this study include nodule within a nodule appearance and the presence of satellite nodules [19].

As Figure 5 shows, the detectability of the lesions varied depending on the particular MR sequence used, with lesions most easily seen on the arterial phase of dynamic gadolinium imaging, where all readers were in agreement. For the remaining sequences, Reader 2 detected a greater number of lesions than Readers 1 and 3. This, however, did not reflect the seniority of the radiologist (Reader 1 being the most experienced) but probably reflects how qualitative analysis in small lesions can be highly subjective. In concordance with the findings in Figure 5, Figure 6 again shows that enhancement in the arterial phase was the most consistent feature with all HCCs enhancing in the present study and with all readers in agreement. For the other 22 imaging features, variable mean confidence ratings were given with wide standard deviations, probably reflecting the heterogeneity of HCCs in general. There have been a number of studies that have shown the value of dynamic gadolinium in the detection of HCCs over T_2 weighted imaging [21, 22]. For example, Fujita et al [21] showed that there was 100% sensitivity for detection of HCC on T_1 weighted dynamic gadolinium imaging compared with a sensitivity of only 68–78% on T_2 weighted imaging. However, other studies [23] have shown that the addition of T_2 weighted imaging to gadolinium-enhanced 3D dynamic imaging can increase reader confidence when there are equivocal findings.

As shown in Table 1, many of the MR features that showed greatest inter-reader consistency (mean discrepancy <1) across all lesions were on the T_1 weighted sequences, with four of the most consistent features being arterial enhancement, heterogeneous enhancement on the arterial phase, absence of fat within the lesion and presence of washout on delayed images. Features such as increased signal intensity, heterogeneity and irregular margin on T_2 all had a mean discrepancy between readers and across all lesions of >1.5. The reason for this difference is unclear but may reflect intrinsic differences in signal to noise ratio of the two acquisitions, making it easier to discern lesions on T_1 weighted sequences. The majority of patients in our study had abnormal background liver texture, which could have influenced the conspicuity of the lesions on the T_1 and T_2 weighted sequences.

In the assessment of MR features associated with vascular invasion, only arterial enhancement could not be included, as this feature was identified in all lesions; hence it was of no use as a predictor of whether vascular invasion was present or not. Out of the subsequent 10 most consistent MR features, washout in the portal venous phase showed a trend towards vascular invasion on histopathology ($p=0.09$); hence this MRI feature may suggest a poorer prognosis. There was approximately 3.9 times greater frequency of vascular invasion in lesions demonstrating washout in the portal venous phase than in lesions not demonstrating this imaging feature. In

addition, a possible but non-significant association with vascular invasion was also suggested with washout in the delayed phase ($p=0.13$). It has been shown that delayed hypointensity of an arterially enhancing mass within the liver is an independent predictor of HCC [24], although contrast enhancement characteristics can be variable [25]. Delayed hypointensity on dynamic contrast enhancement is a more consistent finding in larger tumours [26, 27], which are themselves associated with a poorer prognosis. It is interesting to note that, in the present study, the median size of lesions was larger with vascular invasion. This, however, failed to reach significance, probably because of the small sample size.

Two other features identified in the present study as showing a weak but non-significant correlation with vascular invasion on histopathology ($p \leq 0.18$) included the absence of increased signal intensity on T_1 weighted images and the absence of a rim on the T_1 arterial phase. The latter observation was not a consistent imaging feature, being ranked 13 out of 23 in order of interobserver consistency in our study. Studies have shown that diffuse enhancement with a more prominent rim occurs in only approximately 15% of HCCs [28]. Ishigami et al [29] found that the presence of a pseudocapsule on dynamic MR may correlate with peritumoural sinusoids and/or fibrosis. When compared with HCCs with a true histological fibrous capsule, the incidence of vascular invasion was not significantly different. There are no studies evaluating the correlation between signal intensity on T_1 weighted images and microscopic vascular invasion, although it has been shown that more poorly differentiated HCCs are more likely to be hypo- to isointense on T_1 weighted imaging [30].

Only a few studies [28, 29, 31–33] have attempted to correlate pre-operative imaging with prediction of microvascular invasion in HCC. These studies chiefly used CT during hepatic angiography, CT with arterioportography (CTAP) or superparamagnetic iron oxide-enhanced MRI as imaging modalities [28, 31–33] rather than MRI with dynamic gadolinium. Hence no direct comparison can be made with the present study as none of the 23 imaging factors that we evaluated was addressed. In these studies [28, 31], features found to correlate with microscopic portal invasion included distortion of the tumour corona, tumourous arterioportal shunt, tumour size and a greater ratio of peritumoural haemodynamic change to tumour volume in tumours <3 cm. Three types of area of peritumoural haemodynamic change were identified [31, 32] on CTAP (wedge-shaped, irregular and linear) but no significant difference was found in the frequency of these three types and the presence or absence of minute portal venous or hepatic venous invasion.

As discussed in the introduction, vascular invasion on histopathology is one risk factor that is associated with a greater risk of recurrence and with poorer survival following hepatic resection for HCC [18, 34–37]. The ability to identify pre-operatively imaging characteristics which correlate with the presence of microvascular invasion thus has important prognostic implications. The strongest correlate in our study was the presence of washout within the lesion in the portal venous phase on MRI. This showed a trend towards vascular invasion on histopathology. Clearly, if a consistent imaging feature can be identified on MRI then this would not only predict long-term survival but may also help in stratifying patients for additional treatment such as transcatheter arterial chemoembolisation or adjuvant chemotherapy [36].

There are several limitations to the present study. The authors acknowledge that the sample size was small, with comprehensive liver imaging available at our institution for only 27 lesions. This was because the majority of patients were referred from other institutions where imaging had already been performed. It is calculated that, in order to have 80% power to detect doubling of the rate of vascular invasion from 20% in those where features were absent to 40% where features were present, approximately 180 lesions would have to be evaluated. Clearly this would involve a multicentre study over a prolonged period to achieve this. Second, the present analysis to determine which MR features predicted vascular invasion was somewhat restricted as only 9 out of the 27 lesions demonstrated this particular characteristic.

In conclusion, the present study has shown that HCCs demonstrating washout in the portal venous phase on MRI showed a trend towards vascular invasion on histopathology, with approximately 3.9 times greater frequency of vascular invasion than lesions not demonstrating this imaging feature. Arterial enhancement was a consistent feature seen in all lesions, and thus could not be used as a feature to predict the presence or absence of vascular invasion. A number of other consistent imaging features, such as lack of increased signal intensity within the lesion on T_1 weighted images and the presence of washout in the delayed arterial phase, may also be associated with vascular invasion ($p<0.2$). In addition, the median size of lesions was larger when vascular invasion was present ($p=0.18$). It is possible that a larger study would have demonstrated significance for these findings but this would only be achieved with a multicentre study using uniform protocols. An alternative theory is that prediction of vascular invasion or other markers of poor prognosis is better made with serial imaging where the more typical imaging features for HCC evolve over time. A combination of several imaging features on different sequences (such as arterial enhancement on dynamic gadolinium sequence with high signal intensity on T_2 weighted imaging) rather than an isolated feature on one single sequence may also be of greater value in predicting tumours with poor prognosis. Certainly studies have shown that a combination of MR sequences assists in the diagnosis of HCC [23].

Recently we have added diffusion weighted imaging (DWI) as a routine sequence to our MRI liver protocols. The use of DWI in addition to conventional MRI sequences may assist in the identification of patients with poorer prognosis. There have been no studies to date evaluating the use of DWI in predicting vascular invasion in HCC. However, preliminary studies suggest that a combination of hypovascularity and visibility on DW images can help distinguish poorly differentiated HCCs from well-differentiated HCCs and dysplastic nodules [38].

The authors intend to embark on a larger study of patients with HCC. It is hoped that a larger study will demonstrate a significant correlation between the imaging features identified in the present study and vascular invasion. Attention will be focused on those imaging features (*e.g.* washout in the portal venous phase) identified from the present study that have suggested a correlation with vascular invasion. Serial MRI studies will be reviewed in order to determine if there are changes in signal characteristics with evolution to HCC. Correlation with other prognostic markers such as proliferative indices is also planned to determine whether there is indeed a relationship between specific imaging features and other histopathological outcome predictors.

Ackowledgment

References

1. El-Serag HB, Mason AC. Rising incidence of hepatocellular carcinoma in the United States. N Engl J Med 1999;340: 745–50.
2. Mazziotti A, Grazi GL, Cavallari A. Surgical treatment of hepatocellular carcinoma on cirrhosis: a Western experience. Hepatogastroenterology 1998;45:1281–7.
3. Balsells J, Charco R, Lazaro JL, Murio E, Vargas V, Allende E, et al. Resection of hepatocellular carcinoma in patients with cirrhosis. Br J Surg 1996;83:758–61.
4. Baccarani U, Benzoni E, Adani GL, Benzoni E, Avellini C, Lorenzin D, et al. Superiority of transplantation versus resection for the treatment of small hepatocellular carcinoma. Transplant Proc 2007;39:1898–900.
5. Marelli L, Stigliano R, Triantos C, Senzolo M, Cholongitas E, Davies N. Transarterial therapy for hepatocellular carcinoma: which technique is more effective? A systematic review of cohort and randomized studies. Cardiovasc Intervent Radiol 2007;30:6–25.
6. Choi D, Lim HK, Joh JW, Kim SJ, Kim MJ, Rhim H, et al. Combined hepatectomy and radiofrequency ablation for multifocal hepatocellular carcinomas: long-term follow-up results and prognostic factors. Ann Surg Oncol 2007;14: 3510–18.
7. Ono T, Yamanoi A, Nazmy El Assal O, Kohno H, Nagasue N. Adjuvant chemotherapy after resection of hepatocellular carcinoma causes deterioration of long-term prognosis in cirrhotic patients: metaanalysis of three randomized controlled trials. Cancer 2001;91:2378–85.
8. Butterfield LH. Immunotherapeutic strategies for hepatocellular carcinoma. Gastroenterology 2004;127:S232–41.
9. Llovet J, Ricci S, Mazzaferro V, Hilgard P, Raoul J, Zeuzem S, et al. Sorafenib improves survival in advanced hepatocellular carcinoma (HCC): results of a Phase III randomized placebo-controlled trial (SHARP trial). Proceedings of the ASCO Annual Meeting. J Clin Oncol 2007;Part I. 25:18S.
10. Hecht EM, Holland AE, Israel GM, Hahn WY, Kim DC, West AB, et al. Hepatocellular carcinoma in the cirrhotic liver: gadolinium-enhanced 3D T_1-weighted MR imaging as a stand-alone sequence for diagnosis. Radiology 2006;239: 438–47.
11. Burrel M, Llovet JM, Ayuso C, Iglesias C, Sala M, Miquel R, et al. MRI angiography is superior to helical CT for the detection of HCC prior to liver transplantation: an explants correlation. Hepatology 2003;38:1034–42.
12. Krinsky GA, Lee VS, Thiese ND, Weinreb JC, Rofsky NM, Diflo T, et al. Hepatocellular carcinoma and dysplastic nodules in patients with cirrhosis: prospective diagnosis with MR imaging and explants correlation. Radiology 2001; 219:445–54.
13. Rode A, Bancel B, Douek P, Chevallier M, Vilgrain V, Picaud G, et al. Small nodule detection in cirrhotic livers: evaluation with US, spiral CT and MRI and correlation with pathologic examination of explanted liver. J Comput Assist Tomogr 2001;25:327–36.
14. Pérez-Saborido B, de los Galanes SJ, Menéu-Díaz JC, Romero CJ, Elola-Olaso AM, Suárez YF, et al. Tumour recurrence after liver transplantation for hepatocellular carcinoma: recurrence pathway and prognostic factors. Transplant Proc 2007;39:2304–7.
15. Zhao WH, Ma ZM, Zhou XR, Feng YZ, Fang BS. Prediction of recurrence and prognosis in patients with hepatocellular carcinoma after resection by use of CLIP score. World J Gastroenterol 2002;8:237–42.
16. Nanashima A, Abo T, Sumida Y, Takeshita H, Hidaka S, Furukawa K, et al. Clinicopathological characteristics of patients with hepatocellular carcinoma after hepatectomy: relationship with status of viral hepatitis. J Surg Oncol 2007;96:487–92.
17. Tangkijavanich P, Anukulkarnkusol N, Suqangool P, Lertmaharit S, Hanvivatvong O, Kullavanijaya P, et al. Clinical characteristics and prognosis of hepatocellular carcinoma: analysis based on serum alpha fetoprotein levels. J Clin Gastroenterol 2000;31:302–8.
18. Iwatsuki S, Dvorchik I, Marsh JW, Madariaga JR, Carr B, Fung JJ, et al. Liver transplantation for hepatocellular carcinoma: a proposal of a prognostic scoring system. J Am Coll Surg 2000;191:389–94.
19. Hussain SM, Sondervan PE, Ijzermans JNM, Schalm SW, de Man RA, Krestin G. Benign versus malignant hepatic nodules: MR imaging findings with pathologic correlation. Radiographics 2002;22:1023–39.
20. van den Bos IC, Hussain SM, de Man RA, Zondervan PE, Ijzermans JN, Krestin GP. Primary hepatocellular lesions: imaging findings on state-of-the-art magnetic resonance imaging, with pathologic correlation. Curr Probl Diagn Radiol 2008;37:104–14.
21. Fujita T, Ito K, Honjo K, Okazaki H, MatsumotoT, Matsunaga N. Detection of hepatocellular carcinoma: comparison of T_2-weighted breath-hold fast spin-echo sequences and high-resolution dynamic MR imaging with a phased-array body coil. J Magn Reson Imaging 1999;9:274–9.
22. Hussain HK, Syed I, Nghiem HV, Johnson TD, Carlos RC, Weadock WJ, et al. T_2-weighted MR imaging in the assessment of cirrhotic liver. Radiology 2004;230:637–44.
23. Kim YK, Lee YH, Kim CS, Han YM. Added diagnostic value of T_2-weighted MR imaging to gadolinium-enhanced three-dimensional dynamic MR imaging for the detection of small hepatocellular carcinomas. Eur J Radiol 2007;67: 304–10.
24. Marrero JA, Hussain HK, Nghiem HV, Umar R, Fontana R, Lok AS. Improving the prediction of hepatocellular carcinoma in cirrhotic patients with an arterially enhancing liver mass. Liver Transpl 2005;11:281–9.
25. Lutz AM, Willmann JK, Goepfert K, Marincek B, Weishaupt D. Hepatocellular carcinoma in cirrhosis; enhancement patterns at dynamic gadolinium and superparamagnetic iron oxide-enhanced T_1-weighted MR imaging. Radiology 2005;237:520–8.
26. Bolondi L, Gaiani S, Celli N, Golfieri R, Grigioni WF, Leoni S, et al. Characterisation of small nodules in cirrhosis by assessment of vascularity: the problem of hypovascular hepatocellular carcinoma. Hepatology 2005;42:27–34.
27. van den Bos IC, Hussain SM, Dwarkasing RS, Hop WC, Zondervan PE, de Man RA, et al. MR imaging of

hepatocellular carcinoma: relationship between lesion size and imaging findings, including signal intensity and dynamic enhancement patterns. J Magn Reson Imaging 2007;26:1548–55.

28. Miyata R, Tanimoto A, Wakabayashi G, Shimazu M, Nakatsuka S, Mukai M, et al. Accuracy of preoperative prediction of microinvasion of portal vein in hepatocellular carcinoma using superparamagnetic iron oxide-enhanced magnetic resonance imaging and computed tomography during hepatic angiography. J Gastroenterol 2006;41:987–95.

29. Ishigami K, Yoshimitsu K, Nishihara Y, Irie H, Asayama Y, Tajima T, et al. Hepatocellular carcinoma with a pseudo-capsule on gadolinium-enhanced MR images: correlation with histopathologic findings. Radiology 2009;250:435–43.

30. Kajiwara M. MR imaging of small hepatocellular carcinoma (< or = 20 mm)—correlation with vascularity and histological features. Kurume Med J 1997;44:327–38.

31. Nishie A, Yoshimitsu K, Asayama Y, Irie H, Tajima T, Hirakawa M, et al. Radiologic detectability of minute portal venous invasion in hepatocellular carcinoma. AJR Am J Roentgenol 2008;190:81–7.

32. Nishie A, Yoshimitsu K, Irie H, Tajima T, Hirakawa M, Ishigami K, et al. Radiological detectability of minute hepatic venous invasion in hepatocellular carcinoma. Eur J Radiol 2009;70:517–24.

33. Shirabe K, Kajiyama K, Abe T, Sakamoto S, Fukuya T, Akazawa K, et al. Predictors of microscopic portal vein invasion by hepatocellular carcinoma: measurement of portal perfusion defect area ratio. J Gastroenterol Hepatol 2009;24:1431–6.

34. Abdel-Wahab M, El-Husseiny TS, El Hanafy E, El Shobary M, Hamdy E. Prognostic factors affecting survival and recurrence after hepatic resection for hepatocellular carcinoma in cirrhotic liver. Langenbecks Arch Surg. 2010; 395: 625–32.

35. Shah SA, Cleary SP, Wei AC, Yang I, Taylor BR, Hemming AW, et al. Recurrence after liver resection for hepatocellular carcinoma: risk factors, treatment, and outcomes. Surgery 2007;141:330–9.

36. Cha C, Fong Y, Jarnagin WR, Blumgart LH, DeMatteo RP. Predictors and patterns of recurrence after resection of hepatocellular carcinoma. J Am Coll Surg 2003;197:753–8.

37. Shah SA, Greig PD, Gallinger S, Cattral MS, Dixon E, Kim RD, et al. Factors associated with early recurrence after resection for hepatocellular carcinoma and outcomes. J Am Coll Surg 2006;202:275–83.

38. Muhi A, Ichikawa T, Motosugi U, Sano K, Matsuda M, Kitamura T, et al. High-b-value diffusion-weighted MR imaging of hepatocellular lesions: estimation of grade of malignancy of hepatocellular carcinoma. J Magn Reson Imaging 2009;30:1005–11.